Synthesis and Properties of Liquid Crystalline Polyurethane Elastomers

TAE-JUNG LEE, DONG-JIN LEE, HAN-DO KIM

Department of Textile Engineering, Pusan National University, Pusan, Korea

Received 7 May 1999; accepted 2 November 1999

ABSTRACT: Novel type of mesogenic chain extenders used in this study are *N,N′*-bis(4-hydroxyphenyl)-3,4,3′,4′-biphenyldicarboxyimide (BPDI) and *N,N′*-bis[4-(6-hydroxyhexyloxy) phenyl]-3,4,3′,4′-biphenyldicarboxyimide (BHDI). BHDI has a flexible spacer of 6-methylene units but BPDI does not. The liquid crystalline polyurethane elastomers were synthesized from BPDI or BHDI as a mesogenic chain extender, 4,4′-diphenylmethane diisocyanate, and poly(oxytetramethylene)glycol (MW 1000) as a soft segment. Polyurethane based on BHDI exhibited two melting transitions. However, any melting behavior was not shown in the BPDI-based polyurethanes because of higher melting temperature than decomposition temperature. The composition of polyurethanes was varied as a means of manipulating liquid crystalline behavior and physical properties. The BHDI-based polyurethanes containing above 50 wt % of hard segment content exhibited nematic liquid crystal behaviors. As the hard segment content of the BHDI-based polyurethanes increased, the glass transition temperature (T_g), strength, modulus, and the amount of hydrogen bonding increased. © 2000 John Wiley & Sons, Inc. J Appl Polym Sci 77: 577–585, 2000

Key words: liquid crystalline polyurethane elastomers; soft segment; physical properties; nematic liquid crystal behavior; hydrogen bonding

INTRODUCTION

Recently, thermotropic liquid crystalline polymers having mesogenic units along the main chain have attention as a result of their good mechanical properties and ease of processing. To obtain a useful thermotropic polymer, careful attention must be given to monomer composition. To reduce the melting point of the intractable homopolymers, monomers must be introduced that disrupt the order or regularity of the backbone. Processing temperature can be lowered by copolymerizing the rigid backbone moieties with controlled amounts of a moiety having flexible linkages and/or dissymmetrical units having bulky side groups or kinks. Many studies have been devoted to decrease the melting point to a melt processable temperature range as well as to improve the solubility without destroying the liquid crystal formation.[1–8] For the thermoplastic polyurethanes, because of the strong intermolecular interaction resulting from the hydrogen bonding of urethane linkages, many studies were developed to minimize the hydrogen bonding effects using chain modifications.[9–11]

In liquid crystalline polyurethane elastomers (LCPUEs), it was revealed that the incorporation of mesogenic diol as a chain extender into the backbone could produce liquid crystalline character.[12,13] Because of the liquid crystalline nature of the hard domains, their response to an applied strain should be different from that of hard domains in common polyurethane elastomer, and

Correspondence to: H.-D. Kim.
Contract grant sponsor: Korea Research Foundation.

Journal of Applied Polymer Science, Vol. 77, 577–585 (2000)

such an applied strain may result in a highly oriented and perfect structure. At high elongations, the amorphous soft segments will tend to become anisotropic as well. Thus, this kind of polyurethane may exhibit unusual anisotropic electrical, mechanical properties, leading to future technological application.

Works concerning LCPUEs made from various mesogenic chain extenders were published by Lorentz et al.,[13] Penczek et al.,[14,15] MacKnight et al.,[16] and Chang et al.[17] Lorentz and coworkers reported the mechanical and thermal properties of segmented polyurethane prepared from mesogenic chain extender 4,4′-(ω-hydroxyalkoxy)biphenyl, hexamethylene diisocyanate (HDI) or isophorone diisocyanate (IPDI), and soft segment poly(tetramethylene oxide)diol (PTMG) or polycaprolactone diol. Penczek and coworkers investigated the liquid crystallinity of segmented polyurethanes based on 2,4-TDI, soft segment PTMG, and a mesogenic chain extender 2,2′-bis-(2-hydroxyethoxy)bipheny (BHEBP). MacKnight and coworkers studied the synthesis and the phase behavior of LCPUEs prepared from soft segment PTMG with different chain length, 2,4-TDI or 2,6-TDI, and a chain extender 4,4′-bis-(6-hydroxyhexoxy)bipheny (BHHBP). Chang and coworkers investigated the effect of soft segments on the liquid crystalline behavior of LCPUEs based on PTMG (MW 1000, 2000), 1,10-decanediol as a soft segment, hexamethylene diisocyanate (HDI) or 4,4′-methylenecyclohexyl diisocyanate (H12MDI), and a mesogenic chain extender benzene-1,4-di(4- iminophenoxy-*n*-hexanol).

In this study, we prepared two types of novel mesogenic chain extenders [*N,N′*-bis(4-hydroxyphenyl)-3,4,3′,4′-biphenyldicarboxyimide (BPDI) and *N,N′*-bis[4-(6-hydroxyhexyloxy) phenyl]-3,4,3′,4′-biphenyldicarboxyimide (BHDI)] containing imide unit and synthesized LCPUEs from mesogenic chain extenders BPDI or BHDI, soft segment PTMG (MW 1000), and MDI. The effects of the hard segment content and flexible spacer of a mesogenic chain extender on the liquid crystallinity and properties were investigated. The structures and the thermal properties of all synthesized LCPUEs were examined by using Fourier transform infrared (FTIR) spectroscopy, ^{1}H nuclear magnetic resonance (NMR), differential scanning calorimetry (DSC), polarized microscope with a hot stage, dynamic mechanical thermal analysis (DMTA), and thermogravimetric analysis (TGA). Mechanical and elastic properties were also examined using an Instron (Canton, MA).

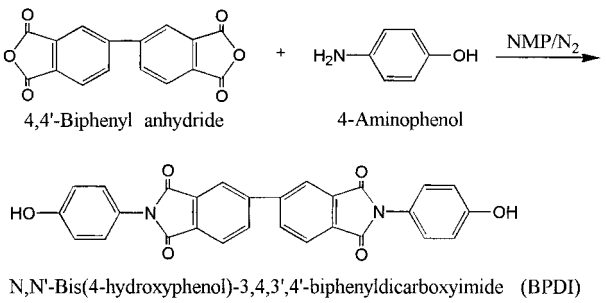

Scheme 1 Reaction scheme of *N,N′*-bis(4-hydroxyphenol)-3,4,3′,4′-biphenyl dicarboxyimide (BPDI).

EXPERIMENTAL

Materials

Poly(tetramethylene)glycol (PTMG, MW 1000; BASF, Carrollton, TX) was used after drying in vacuum at 80°C. 1,4-Diphenylmethane diisocyanate (MDI; Aldrich, Milwaukee, WI) was used without further purification. 1,4-Aminophenol (Aldrich), 4,4′-biphthalic anhydride (Tokyo Kasei. Co.), and 6-chloro-1-hexanol (Aldrich) were used as received. *N,N′*-Dimethylformamide (DMF) and *N*-methyl-2-pyrrolidone (NMP) were dried over molecular sieves and distilled under reduced pressure.

Synthesis and Identification of Chain Extender BPDI

1,4-Amino phenol (0.046 mol : 5.019 g) and 4,4′-biphthalic anhydride (0.023 mol : 6.744 g) were mixed in 35 mL of NMP. The mixture was reacted for 14 h at 90°C and then poured into nonsolvent methanol. The precipitate BPDI was filtered off and recrystallized from DMF. The reaction was shown in Scheme 1. Yield 65%. Mp 141°C, ^{1}H-NMR (DMSO-*d6*, 300 MHz): BPDI, δ 6.87–6.91 (4H, d), 7.19–7.23 (4H, d), 8.00–8.03 (2H, d), 8.26–8.29 (4H, d), 9.69 (2H, s)

Synthesis and Identification of Chain Extender BHDI

BHDI was synthesized without any base and catalyst by the method previously reported.[18,19] The BPDI (0.0013 mol : 0.62 g)/DMF (40 mL) solution was placed in a 250-mL three-necked flask equipped with a dropping funnel and a reflux condenser and was heated to 80°C. Then, 6-chloro-1-hexanol (0.0026 mol : 0.36 g) was added dropwise. The reaction was continued by

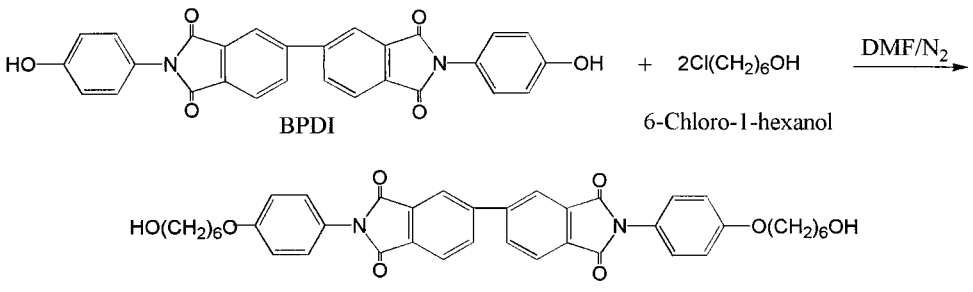

N,N'-Bis[4-(hydroxyhexyloxyl)phenyl]-3,4,3',4'-biphenyldicarboxyimide (BHDI)

Scheme 2 Reaction scheme of *N,N′*-bis[4-(6-hydroxyhexyloxy)phenyl]-3,4,3′,4′-biphenyldicarboxyimide (BHDI).

refluxing for 15 h and poured into nonsolvent water. The precipitated material BHDI was filtered off and recrystallized from DMF. The reaction is shown in Scheme 2. Yield 38%. Mp 110°C. ^{1}H-NMR (DMSO-*d6*, 300 MHz): BHDI, δ 1.13–1.25 (16H, m), 3.46–3.64 (4H, m), 4.05–4.09 (4H, t), 4.25–4.29 (2H, t), 6.92–6.95 (4H, d), 7.02–7.06 (4H, d), 7.11–7.14 (2H, d), 7.18–7.23 (4H, d).

Synthesis of Liquid Crystalline Polyurethane Elastomers

The general reaction routes for two types of the liquid crystalline polyurethane elastomers (LCPUEs) synthesized in this study are shown in Scheme 3. To a 250-mL four-necked flask equipped with a condenser, thermometer, magnetic stirrer, and nitrogen inlet–outlet were added PTMG (MW 1000; 0.00033–0.00084 mol), MDI (0.0011 mol), and DMF (15–20 mL). The reaction mixture was stirred for 2 h at 80 under nitrogen gas. Then DMF (15 mL) and mesogenic diol (BPDI or PHDI; 0.00026–0.00077 mol) were added, and the reaction was continued for 24 h at 100°C. DMF was added as the reaction proceeded to keep the solution viscosity low enough to allow stirring. The yellow polymer was precipitated out by pouring the reaction mixture into methanol. The precipitated polymer was filtered off and dried in vacuum at 60°C.

The mesogenic diol, BPDI, was used as a chain extender for preparing polyurethane elastomer MP samples, and BHDI was used for preparing polyurethane elastomer MH samples. The various materials synthesized in this way are identified in Table I.

Measurements

^{1}H-NMR

The ^{1}H-NMR spectra were recorded on a Varian (Lexington, MA) Unity Plus 300 spectrometer. The concentration of the polymer solutions was about 15%. The NMR tube (5 mm) was used in a spinning mode. The samples were prepared by using DMSO-*d6* and hexamethylenedisiloxane (HMDS) as a internal reference.

Infrared Spectroscopy

To confirm the structure of the synthesized mesogenic chain extenders and polymers, infrared

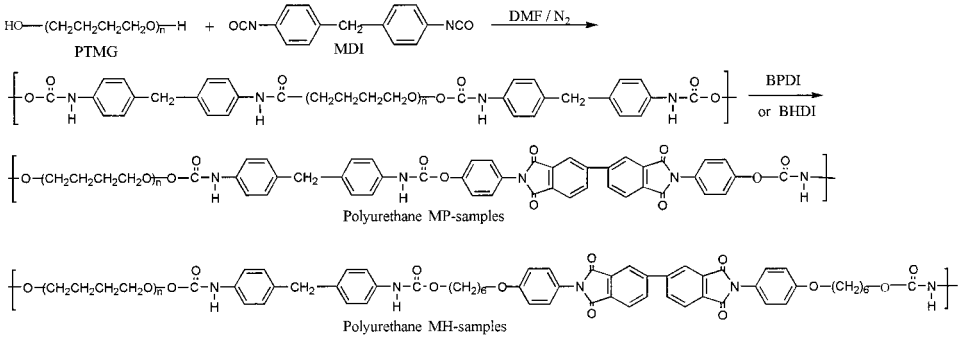

Scheme 3 Synthesis of liquid crystalline polyurethane elastomers.

Table I Properties of MP and MH Samples

Sample	Composition as Molar Ratio MDI/BPDI/PTMG (BHDI)	Hard Segment Contents (%)	η inh[a] (dL/g)	Yield (%)	Weight Loss (°C)[b]		
					10%	20%	30%
MP-35	1.0/0.30/0.70	35	0.64	70	280.33	315.42	333.44
MP-45	1.0/0.45/0.55	45	0.62	78	295.26	326.55	355.78
MP-65	1.0/0.70/0.30	65	0.55	70	320.85	351.68	375.52
MH-35	1.0/0.24/0.76	35	0.69	76	284.41	319.33	345.22
MH-50	1.0/0.44/0.56	50	0.61	80	300.65	331.12	359.17
MH-65	1.0/0.64/0.36	65	0.59	79	334.50	357.24	384.79

[a]Solvent: DMF; concentration: 0.5 g/dL.
[b]TGA measurements, at a heating rate of 10°C/min under nitrogen atmosphere.

spectroscopy was performed using a FTIR spectrometer (Impact 400D; Nicolet, Northvale, NJ). For each sample, 32 scans at 2 cm^{-1} resolution were collected in the absorption mode. From FTIR spectra, the degree of hydrogen bonding of hard segments was examined. The spectra were analyzed using a curve-resolving technique based on a linear least-squares analysis to fit a combination of the Lorentzian and Gaussian curve shape.

Differential Scanning Calorimetry

The thermal behavior of samples was examined by using a DSC 220C (Seiko) at a heating rate of 10°C/min under a nitrogen atmosphere.

Polarizing Optical Microscopy

Optical textures were observed with an Zeiss (Thornwood, NY) polarizing optical microscope equipped with a Linkam THMS 600 hot stage.

Thermal Gravimetry

The measurements of thermostabilities were performed on a Du Pont (Wilmington, DE) 9900 TGA at a heating rate of 10°C/min under a nitrogen atmosphere.

Dynamic Mechanical Measurement

The dynamic mechanical thermal behaviors of polymers were measured by a DMTA (MkIII; Rheometric Scientific, Piscataway, NY). The DMTA was operated from −80 to 250°C at a heating rate of 3°C/min and the frequency of 2 Hz. The films with dimensions of $8 \times 3 \times 0.5$ mm^3 were prepared by solvent casting for all DMTA measurements.

Tensile Test

Tensile testing was carried out with a Tinius Oslen 1000 on dumbbell specimens of cross-sectional area 3×0.5 mm^3 at room temperature. The crosshead speed was 20°C/min.

Tensile–Retraction Test

This test was carried out with the same tester as above, at room temperature. The sample was clamped in the tester and was subjected to successive maximum 300%.

RESULTS AND DISCUSSION

The structure of the resulting polyurethane was identified with FTIR spectroscopy. As shown in Figure 1, the typical IR spectrum of the sample MH-65 at room temperature showed the bands near 3330 cm^{-1} (N–H stretch), 1700 cm^{-1} (C=O stretch), 1540 cm^{-1} (C–N–H bending), and 1280 cm^{-1} (N–C–O stretch).

Both of the BPDI-based MP samples and BHDI-based MH samples had a constant soft segment molecular weight (MW 1000) but various hard segment content from 35 to 65%. The structural difference between BPDI and BHDI is that BHDI has a flexible spacer of 6-methylene units, but BPDI does not. The inherent viscosities of MP and MH samples synthesized in this study were

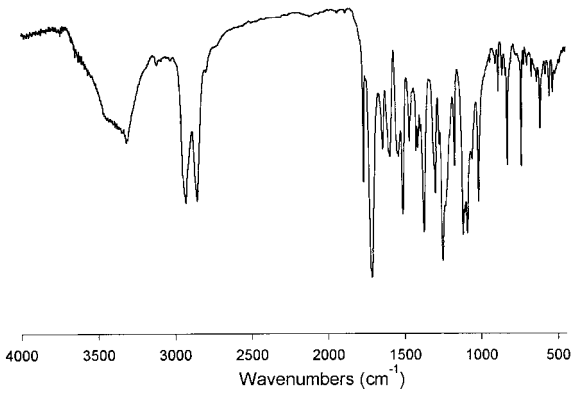

Figure 1 FTIR spectrum of a typical sample MH-65 at room temperature.

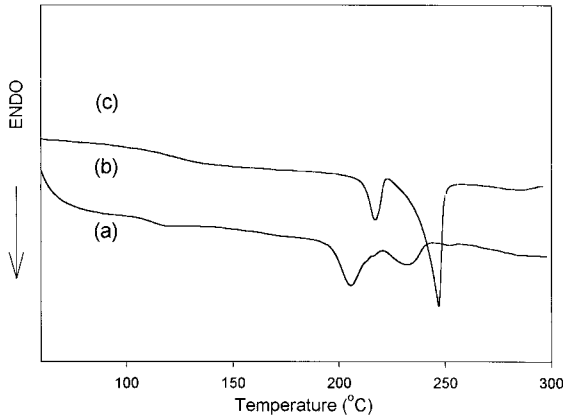

Figure 3 DSC high-temperature thermograms for samples (a) MH-35, (b) MH-50, and (c) MH-65.

in the range of 0.55–0.64 and 0.51–0.65 dL/g, respectively (Table I).

Figure 2 shows the DSC/TGA curves of a representative sample MP-65. By the thermal analysis of DSC/TGA curves, it was found that the endothermic peak of DSC corresponds to the decomposition temperature. The melting temperatures of all MP samples were not detected, indicating higher melting temperature than decomposition temperature. Therefore, the thermotropic liquid crystalline behavior of all MP samples synthesized in this study could not be observed. The 10, 20, and 30% weight loss temperatures of MP samples were summarized in Table I.

The DSC thermogram of the samples MH-35, -50, -65 are presented in Figure 3. Two endothermic peaks for these samples were detected at 207 and 234°C, 215 and 246°C, 211 and 254°C, respectively. The peak appearing at the lower temperature might be associated with a crystal–crystal transition since the polarizing microscope observation did not reveal any crysta–mesophase transition in this temperature range. The endothermic peaks positioned at the higher temperature were found to the crystal–mesophase transition temperature confirmed by the polarizing microscope. As listed in Table II, the main endothermic peaks shifted to higher temperature and the heat of fusion (ΔHm) increased as the hard segment content increased from 35 to 65%. The morphological texture of a typical sample prepared, MH-50, was studied as a function of temperature using a polarizing optical microscope mounted with a hot stage. Microphotographs taken at different temperatures during the heating and cooling experiments are shown in Figure 4. The nematic textures were observed at 240°C on heating and at 206°C on cooling. Similar textures were also found in the MH-65 sample. However, the sample MH-35 containing 35% of hard segment content did not show liquid crystalline behavior. The isotropic temperature (T_i) of MH samples confirmed by the polarizing microscope also increased with increasing the hard segment content (see Table II).

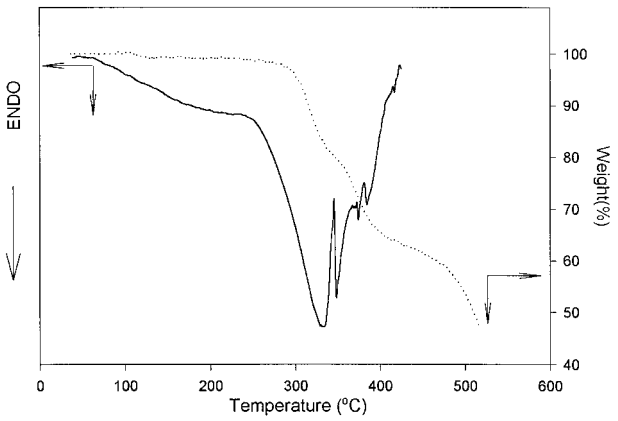

Figure 2 (a) DSC thermogram and (b) thermogravimetry of a typical sample MP-65.

Generally, the hydrogen bonding of polyurethane is investigated by FTIR spectroscopy. There is some absorption of the carbonyl bands of urethane groups as reported by Zharkov and coworkers.[20] The peak at 1730 cm^{-1} was a characteristic of the carbonyl group remaining free. The peak at 1702 cm^{-1} was assigned to the absorption of urethane groups involved in the strongest ordered hydrogen bonds, and the peak at 1713 cm^{-1} was assigned to weaker interaction and less or-

Table II Thermal Properties and K Value of MH Samples

Samples	DSC (°C)[a]						Phase Transition (°C)[b]		Area of Free C=O	Area of HB C=O	*K* Value[c]
	T_g	T_{m1}	T_{m2}	T_i	ΔH_{m1}	ΔH_{m2}	T_m	T_i			
MH-35	110	207	234	—	7.3	7.9	196	—	12.5	22.5	1.8
MH-50	120	215	246	—	5.8	21	206	238	13.2	31.7	2.4
MH-65	124	211	254	—	4.8	22.9	201	246	12.7	40.6	3.2

[a]DSC measurement, at a heating rate of 10°C/min.
[b]Obtained by polarizing microscopy with a hot stage.
[c]*K* = (area of H-bonded C=O/area of free C=O). Based on a linear least-squares analysis to fit the two Gaussian curve shape.

dered structures. The IR spectra of the carbonyl bands of the typical sample MH-50 at various temperatures are shown in Figure 5. The spectrum of MH-50 obtained at room temperature exhibited two absorption peak near 1702 and 1713 cm^{-1}. As the temperature increased, the intensity of the less ordered hydrogen-bonded carbonyl band near 1730 cm^{-1} significantly increased as shown in Figure 5a–5e. The ordered hydrogen-bonded carbonyl bands near 1702 cm^{-1} decreased with increasing temperature from room temperature to 250°C. This result indicates that the ordered hydrogen-bonded carbonyl bands near 1702 cm^{-1} are transformed into free carbonyls and less ordered hydrogen-bonded carbonyl groups with increasing temperature. When the sample MH-50 was heated to isotropic temperature 280°C, the hydrogen-bonded carbonyl band still existed near 1713 cm^{-1}.

To analyze the FTIR data quantitatively, curve fitting is used to resolve the carbonyl region into its constituents. The dominance of the hydrogen-bonded carbonyl band indicates that a large fraction of the hard segments are hydrogen bonded.[21,22] Figure 6 shows that there are two

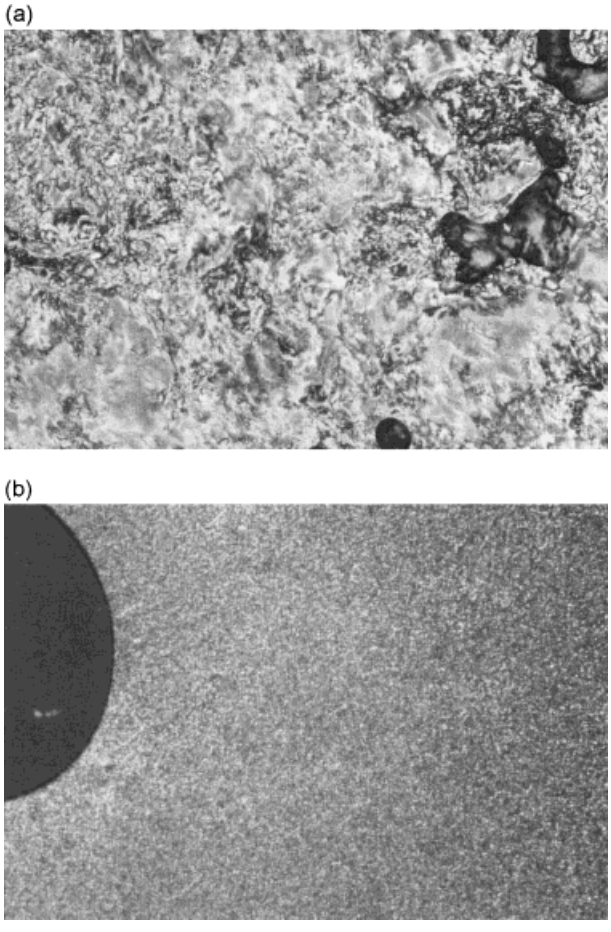

Figure 4 Polarizing optical micrographs of the sample MH-50. (a) Mesophase at 240°C on heating (b) at 206°C on cooling.

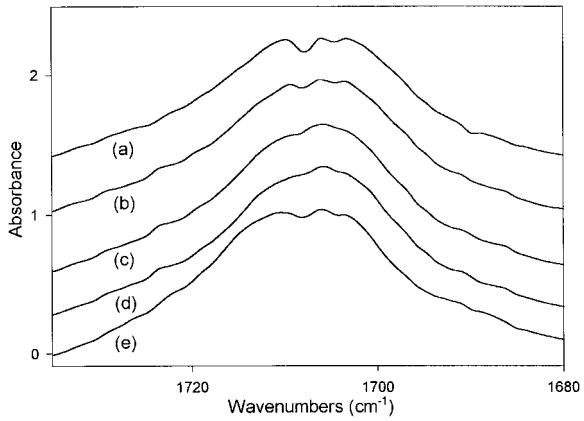

Figure 5 FTIR spectra of a typical sample MH-50 at various temperature.

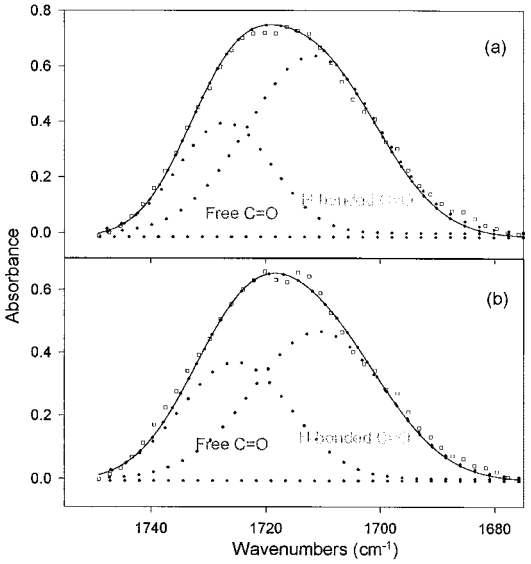

Figure 6 Curve-fitting analysis of the C=O stretching region for samples (a) MH-65 and (b) MH-50.

different bands that correspond to the ordered hydrogen-bonded groups near 1702 cm^{-1} and the free carbonyl groups near 1730 cm^{-1} for the MH-65 and MH-50 samples. The hydrogen-bonded carbonyl region of the MH-65 sample is larger than that of the MH-50 as shown in Figure 6. Table II summarizes the detail results of the curve fitting of the carbonyl region with the various hard segment contents. As the hard segment content increases, the value of K (area of hydrogen-bonded carbonyl region/area of free carbonyl region) increased. In an earlier work of similar polyurethane, the K value also increased with increasing the hard segment content.[23]

For polyurethane elastomers, better phase separation and a more developed reinforcing hard-domain structure will increase the stiffness of the material and improve its tensile strength.[24] Ng et al.[25] used DMTA method to characterize several linear segmented polyurethanes of well-defined hard and soft segment molecular weights and molecular weight distributions. Chen et al.[26] showed that increasing the hard and soft segment length for a fixed hard/soft segment composition ratio provides more complete phase separation, an increase in modulus, and a decrease in soft domain T_g (due to purer soft phase).

Figure 7 illustrates the dynamic mechanical storage modulus of the samples MH-35, -50, and -65. The modulus of the almost plateau region increased and extended to higher temperature as

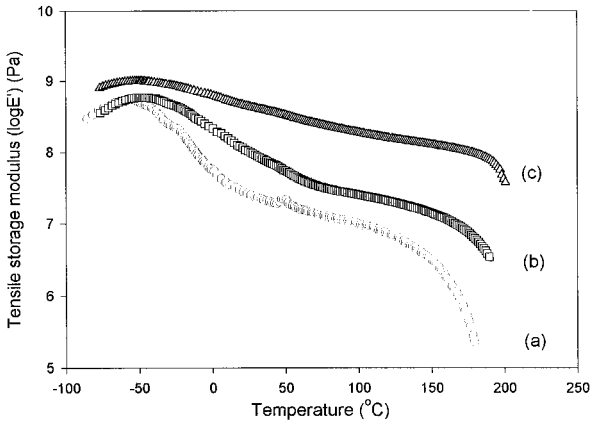

Figure 7 Tensile storage modulus for samples (a) MH-35, (b) MH-50, and (c) MH-65.

the hard segment content increased. Figure 8 shows that tan δ curves of the samples MH-35, -50, and -65 increase with temperature. As the hard segment content increased, the α-type transition peak shifted to higher temperature and the β-type transition peak corresponding to the glass transition of PTMG soft segment phase also increased and broadened. These phenomena indicate a partially phase-mixed morphology with increasing hard segment content.

The stress–strain properties of the MH-35, -50, and -65 samples are shown in Figures 9 and 10. Figure 9 shows that tensile strength and modulus increased with increasing the hard segment content. The MH-35 sample had good elastomeric behavior. However, the liquid crystalline polyurethane elastomer MH-50 and -65 samples showed hard plastic instead of elastic behavior. Therefore, it

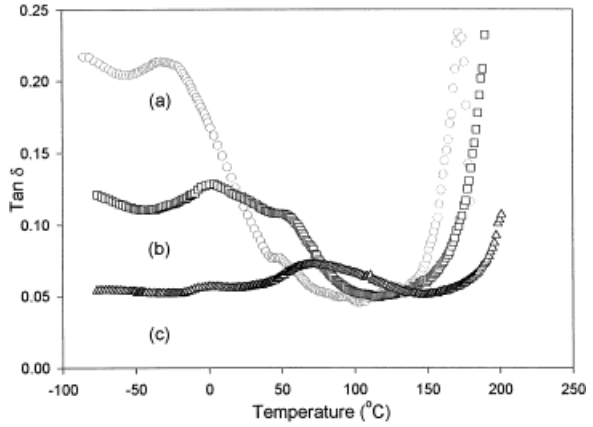

Figure 8 Tan δ for samples (a) MH-35, (b) MH-50, and (c) MH-65.

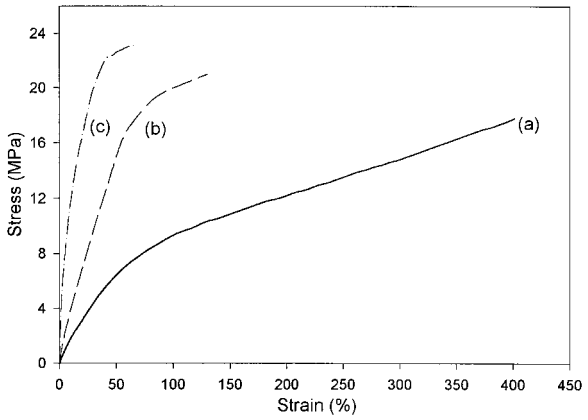

Figure 9 The tensile stress as a function of strain for samples (a) MH-35, (b) MH-50, and (c) MH-65.

was concluded that the content of mesogenic chain extender (hard segment) was the important factor to control the elastic behavior. Figure 10 shows the tensile retraction curves of three cycles for a typical sample MH-35. In general, the segmented thermoplastic elastomers require a greater stress to produce a given elongation in the first extension than during subsequent extensions. As the elongation continues, the hard segments become progressively oriented the stretch direction. As shown in Figure 10, the MH-35 sample also required greater stress to produce a given elongation in the first extension than during subsequent extensions. The polyurethane prepared here gave different elastic behaviors with the numbers of cycle. It was suggested that stress-induced ordering of MH-35 sample may be occurred during hysteresis test, thereby possibly restricting the viscoelastic recovery of the material.

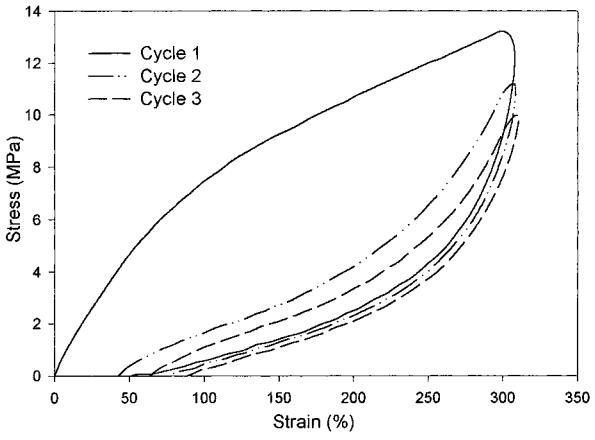

Figure 10 Stress–strain hysteresis curve of a typical sample MH-35.

CONCLUSION

Liquid crystalline polyurethane elastomers based on PTMG (MW 1000) as soft segment, MDI as diisocyanate, and BPDI (or BHDI) containing imide linkage as mesogenic chain extender were synthesized and characterized by FTIR, ^{1}H-NMR, DSC, TGA, DMTA, and polarizing microscopy.

The BPDI-based MP samples exhibited one endothermic peak on DSC thermogram. TGA data revealed that the decomposition temperature was the same as that of polyurethanes. The high melting point of the MP samples is due to the rigid chain in mesogenic diol, which corresponded to the decomposition temperature of the polyurethane.

The BHDI-based MH samples that have a flexible spacer produced two melting points. The higher main melting point increased with increasing hard segment contents. For these MH samples, the main relaxation transition (T_g) shifted to a higher temperature as the hard segment contents increased. The MH-50 and -65 samples showed a nematic textures but the sample MH-35 did not show liquid crystal behavior. The value of K (area of hydrogen-bonded C=O/ area of free C=O) increased with increasing the hard segment content. As the hard segment content, tensile strength, and modulus of MH samples synthesized in this study increased, however, tensile retraction decreased.

REFERENCES

1. Majnusz, J.; Catala, J. M.; Lenz, R. W. Eur Polym J 1983, 19, 1043.
2. Iimura, K.; Koide, N. Ohta, R.; Takeda, M. Makromol Chem 1981, 182, 2563.
3. Jedlinski, Z.; Franek, J.; Kuziw, P. Makromol Chem 1986, 187, 2317.
4. Smyth, G.; Valles, E. M.; Pollack, S. K.; Grebowicz, J.; Stenhouse, P. J.; Hsu, S. L.; MacKnight, W. J. Macromolecules 1990, 23, 3329.
5. Krigbaum, W. R.; Hakemi, H.; Kotek, R. Macromolecules 1985, 18, 965.
6. Dicke, H. R.; Lenz, R. W. J Polym Sci Polym Chem Ed 1983, 21, 258.
7. Kricheldorf, H. R.; Awe, J. Makromol Chem 1989, 190, 2579.
8. Krigbaum, W. R.; Preston, J.; Ciferri, A.; Shufan, Z. J Polym Sci Polym Chem Ed 1987, 25, 652.
9. Iimura, K.; Koide. N.; Tanabe, H.; Takeda, M. Makromol Chem 1981, 182, 2569.

10. Lee, D.-J.; Lee, J.-B.; Koide, N.; Akiyama, E. T.; Uryu, T. Macromolecules 1998, 31, 975.
11. Lee, D.-J.; Uryu, T. Macromolecules 1998, 31, 7142.
12. Mormann, W.; Benadda, S. Polym Prepr (Am. Chem Soc Div Polym Chem) 1993, 34, 739.
13. Lorenz, R.; Els, M.; Haulena, F.; Schmitz, A.; Lorenz, O. Angrew. Makromol Chem 1990, 180, 51.
14. Penczek, P.; Frisch, K. C.; Szczepaniak, B.; Rudnik, E. J Polym Sci Part A Polym Chem 1993, 31, 1211.
15. Szczepaniak, B.; Frisch, K. C.; Penczek, P.; Mejsner, J.; Leszczynska, I.; Rudnik, E. J Polym Sci Part A Polym Chem 1993, 31, 3223.
16. Tang, W.; Farris, R. J.; MacKnight, W. J.; Eisenbach, C. D. Macromolecules 1994, 27, 2814.
17. Sun, S.-J.; Hsu, K.-Y.; Chang, T.-C. J Polym. Sci Part A Polym Chem 1995, 33, 787.
18. Lee, J. B.; Kato, T.; Yoshida, T.; Uryu, T. Macromolecules 1993, 26, 4986.
19. Lee, J. B.; Kato, T.; Ujiie, S.; Iimura, K.; Uryu, T. Macromolecules, 1995, 28, 2165.
20. Zharkov, V. V.; Strikovski, A. G.; Verteletskaya, T. E. Polym Sci 1992, 34. 142.
21. Sung, C. S. P.; Schneider, N. S. Macromolecules 1975, 8, 68.
22. Wang, C. B.; Cooper, S. L. Macromolecules 1983, 16, 775 .
23. Kim, H. D.; Lee, T. J.; Huh, J. H.; Lee, D. J. J Appl Polym Sci 1999, 73, 345.
24. Speckhard, T. A.; Cooper, S. L. Rubber Chem Technol 1986, 59, 405.
25. Ng, H. N.; Allegrezza, A. E.; Seymour, R. W.; Cooper, S. L. Polymer 1973, 14, 255.
26. Chen, W.; Frisch, K. C.; Kenney, D. J.; Wong, S. J. M. S. Pure Appl Chem 1992, 29, 567.